Hairpin Formation within the Human Enkephalin Enhancer Region. 1. Kinetic Analysis†

A. Marquis Gacy‡ and Cynthia T. McMurray*,‡,§

Department of Biochemistry and Molecular Biology and Department of Pharmacology, Mayo Foundation and Mayo Graduate School, Rochester, Minnesota 55905

Received April 21, 1994; Revised Manuscript Received July 20, 1994®

ABSTRACT: The 3′–5′ cyclic AMP inducible enhancer region of the human enkephalin gene is located within an imperfect palindrome of 23 base pairs, located from −106 to −84 base pairs upstream of the transcriptional start site. Recent evidence has indicated that hairpin formation within this region may be involved in transcriptional regulation of the human proenkephalin gene. A 23-bp synthetic oligonucleotide of this region has been shown to undergo a reversible conformational change from a duplex to a cruciform structure of two hairpins [McMurray, C. T., Wilson, W. D., & Douglass, J. O. (1991) *Proc. Natl. Acad. Sci. U.S.A. 88*, 666]. Our current studies explore the kinetics and activation energies of the hairpin to duplex transitions of synthetic oligonucleotides under a variety of conditions. Ultraviolet spectroscopic data collected over a range of pH values, ionic strengths, and temperatures are used to determine the reaction rates and activation energies of the hairpin to duplex reaction. The rate of formation of a duplex from two hairpins is a slow second-order process, dependent on both pH and ionic strength. The return from the hairpin state to the duplex state occurs with a high activation energy of 22–41 kcal/mol strand, depending on the conditions. Pseudo-first-order reaction conditions indicate that one of the hairpins, the AC hairpin, is the rate-limiting reactant. These results suggest a model by which the formation of a cruciform might regulate transcription.

The transcriptional regulation of neuropeptide genes is a model system used to link cell surface effects to gene regulation through second messenger production pathways (Goodman, 1990). These pathways ultimately lead to the activation of transcriptional proteins or complexes that interact with specific enhancers. The human enkephalin gene, which encodes the neuroendocrine peptide precursor proenkephalin, can be regulated through at least three pathways: cAMP,[1] Ca^{2+}, and phorbol ester (Comb et al., 1986; Giraud et al., 1991; MacArthur et al., 1993). Transcriptional induction of the enkephalin gene by these second messengers has been mapped to a 23-bp imperfect palindromic DNA sequence located −84 to −106 bp upstream of the transcriptional start site (Figure 1A) (Comb et al., 1986). Two cAMP response elements in the enhancer region, termed CRE-1 and CRE-2, are both necessary for a complete cAMP response (Comb et al., 1988). The response to cAMP within this region can be mediated by members of the AP-1 (Kobierski et al., 1991; Sonnenberg et al., 1989) and CREB (Huggenvik et al., 1991; Spiro et al., 1993) protein families, although only CRE-2 contains a potential AP-1 or CREB binding site. One suggested model for the transcriptional activation requirement of CRE-1 is its potential to form a stable hairpin structure with CRE-2, due to its partially palindromic sequence. The two hairpins are called the AC hairpin and the GT hairpin, named for the AC and GT mismatches in each hairpin (Figure 1A). The NMR structures of each hairpin are reported in the accompanying paper (McMurray et al., 1994a). The GT hairpin, which contains both CRE-1 and CRE-2, is a strong binding site for CREB (Spiro et al., 1993).

Several lines of evidence have suggested that cAMP-induced transcriptional regulation of the proenkephalin gene involves a hairpin structure. A 23-bp enkephalin enhancer oligonucleotide duplex can reversibly convert to two hairpins under specific solution conditions, stabilized partly by a pH-dependent increase in the stability of the AC hairpin (McMurray et al., 1991). Within the enkephalin enhancer, mutations that stabilize or destabilize a potential cruciform structure increased or decreased levels of transcription, respectively, without affecting protein binding (Comb et al., 1988). CREB binds to the proenkephalin enhancer in striatum nuclear extracts, while AP-1 does not (Konradi et al., 1993). CREB binds more strongly to the GT hairpin than it does to either the native, perfectly hydrogen-bonded enhancer duplex or the AC hairpin. In addition, CREB's ability to activate proenkephalin transcription requires both CRE-1 and CRE-2, even though CREB does not bind CRE-1 (Spiro et al., 1993).

DNA structural changes have been linked to the transcriptional regulation of other genes, both prokaryotic and eukaryotic. Sequence specific regulatory proteins such as λcro (Brennan et al., 1990; Lyubchenko et al., 1991), TFIIIA (Bazett-Jones & Brown, 1989; Nickol & Rau, 1992), and AP-1 (Kerppola & Curran, 1991) can bend synthetic DNA enhancers *in vitro*. In certain *Escherichia coli* genes, bending has been shown to actively influence gene transcription (Pérez-Martín & Espinosa, 1993). Cruciforms inserted at transcriptional start sites reduced transcription through negative supercoiling-induced cruciform formation (Horwitz & Loeb, 1988). The high-mobility group-1 protein (HMG1), a

† This work was supported by the Mayo Foundation, the Eagle's Cancer Fund, and National Science Foundation Grant IBN 9222848 to C.T.M.

* Author to whom correspondence should be addressed.

‡ Department of Biochemistry and Molecular Biology.

§ Department of Pharmacology.

® Abstract published in *Advance ACS Abstracts,* September 15, 1994.

[1] Abbreviations: bp, base pair; cAMP, cyclic adenosine monophosphate; CRE, cAMP response element; CREB, CRE binding protein; AC hairpin, 23-bp oligonucleotide strand of the enkephalin enhancer that forms a hairpin containing two AC mismatches; GT hairpin, 23-bp oligonucleotide strand of the enkephalin enhancer that forms a hairpin containing two GT mismatches; HMG1, high-mobility group-1 protein; PKA, protein kinase A; Pipes, piperazine-*N*,*N*′-bis(2-ethanesulfonic acid); Pipes-00, 10 mM Pipes and 0.1 mM EDTA; Pipes-10, 10 mM Pipes, 0.1 mM EDTA, and 100 mM NaCl.

0006-2960/94/0433-11951$04.50/0

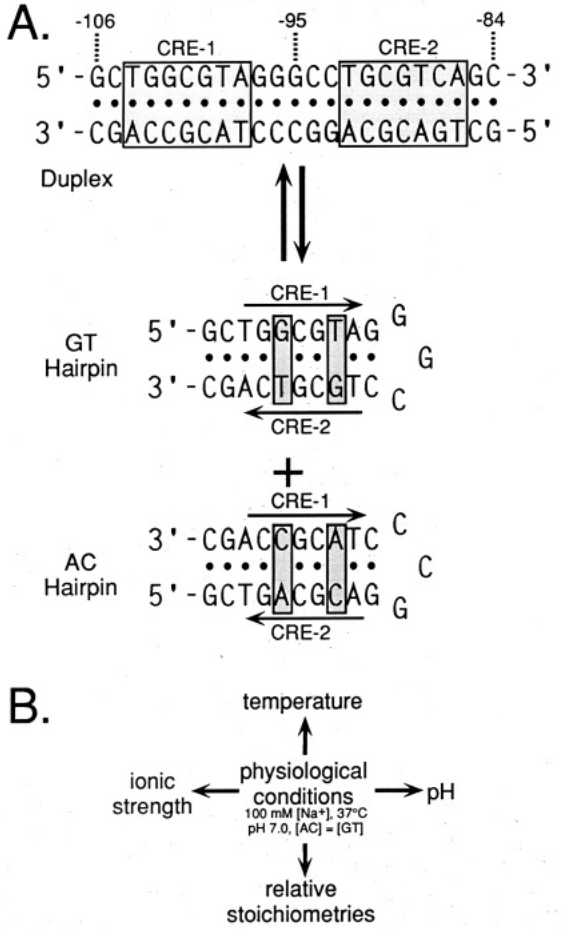

FIGURE 1: (A) Schematic representation of the hairpin to duplex transition of the enkephalin enhancer. The two 23-bp hairpins, the AC and GT hairpins, form the perfectly paired duplex. The boxed areas on the linear duplex indicate CRE-1 and CRE-2. The boxed areas on the hairpins indicate the mismatched pairs. The arrows along the hairpins indicate the direction of CRE-1 and CRE-2 in each hairpin. (B) Conditions used to probe the properties of the hairpin to duplex transition.

ubiquitous eukaryotic nuclear protein, specifically binds to cruciforms in a sequence-independent manner (Bianchi et al., 1989). Finally, the viral RNA polymerase of bacteriophage N4 requires a hairpin structure in the template strand of the promoter for recognition (Glucksmann et al., 1992).

In this paper, we study the thermodynamic and kinetic properties of the 23-bp enkephalin enhancer's hairpin to duplex transition using ultraviolet spectroscopic methods. We altered the pH, ionic strength, relative stoichiometry, and temperature to determine how these conditions could affect the hairpin to duplex transition (Figure 1B). The results were used to determine if the reversible DNA secondary structural change from two stable hairpins back to a duplex displayed properties consistent with a transcriptional regulatory switch. Our studies show that the hairpin state is very stable and slow to transit back to the duplex state. The kinetics of the hairpin to duplex reaction is pH and ionic strength dependent, and the AC hairpin, whose stability is pH sensitive, is rate limiting. The activation energy required to return to the duplex state is high, 25–40 kcal/mol, dependent on the conditions. These data suggest that the proenkephalin enhancer hairpin state has a long lifetime and does not easily switch back to the duplex conformation. The slow rate and high activation energy of the hairpin to duplex reaction further indicate that the cruciform has the potential to regulate the rate of transcription, even after conditions favor return to the duplex state.

EXPERIMENTAL PROCEDURES

Oligonucleotide Synthesis and Preparation. The two single-stranded oligonucleotides, the GT strand (5′-GCTGGCG-TAGGGCCTGCGTCAGC-3′) and its complementary AC strand (5′-GCTGACGCAGGCCCTACGCCAGC-3′), were synthesized and purified by Genetics Design Inc. (Houston, TX) and Oligos Etc. Inc. (Wilsonville, OR), using standard solid state synthesis techniques. (Hairpin mismatches are underlined.) When necessary, oligonucleotides were further purified by passage through 3–6 10 mL desalting columns. Purity was confirmed by gel electrophoresis and NMR (Spiro et al., 1993). The purified oligonucleotides were lyophilized, resuspended in nanopure water, and stored at −20 °C until use.

The molar extinction coefficient of single-stranded oligomers at 260 nm and 25 °C (ϵ_{260}) was calculated by the nearest neighbor method (Cantor & Tinoco, 1965; Cantor et al., 1970). For the GT strand, the ϵ_{260} per nucleotide is 9091 M^{-1} cm^{-1} and the ϵ_{260} per oligomer strand is 209 093 M^{-1} cm^{-1}. For the AC strand, the ϵ_{260} per nucleotide is 9026 M^{-1} cm^{-1} and the ϵ_{260} per oligomer strand is 207 598 M^{-1} cm^{-1}. The concentration of strand stock samples was determined by melting each strand to remove potential secondary structure (see below), extrapolating the absorbance at high temperature to 25 °C, and dividing the extrapolated absorbance by the calculated extinction coefficients.

The GT and AC strands in the hairpin conformation are called the GT hairpin and the AC hairpin, respectively. Duplex formation was performed by equimolar, quantitative mixing of each hairpin. The completeness of duplex formation was confirmed by gel electrophoresis and thermal melting analysis. Hairpin or duplex samples were diluted to the desired concentration in either low-salt buffer [10 mM Pipes and 0.1 mM EDTA (Pipes-00)] or high-salt buffer [10 mM Pipes, 0.1 mM EDTA, and 100 mM NaCl (Pipes-10)]. The pH of each buffer was adjusted to pH 6.0, 7.0, or 8.0, as required. Oligonucleotides were heated to 67 °C for 45 min and placed on ice for 10 min. Rapid cooling traps the hairpin conformation since it forms quickly, minimizing the formation of potential multistrand aggregates (such as homoduplex formation). The samples were then allowed to equilibrate to the appropriate temperature for 0.5 h before use.

Gel Electrophoresis. Nondenaturing polyacrylamide gels were made according to standard methods (Chory, 1993) with modifications in the buffers. Oligonucleotides were separated on a 30 cm × 14 cm × 1 mm nondenaturing 12% polyacrylamide/0.3% bisacrylamide gel buffered in 100 mM Pipes and 0.1 mM EDTA at pH 7.0. Samples were diluted into a buffer of 10 mM Pipes, 0.1 mM EDTA, and 80 mM NaCl, containing 10% glycerol. No dye was added to the samples; instead, a bromophenol blue marker was loaded into a separate well to monitor mobility. The gel was run under a constant voltage of 200 V until the desired separation was achieved. After separation, the gel was soaked in a 0.1% ethidium bromide solution for 10 min. The gel was photographed on an ultraviolet light transilluminator. The photograph was scanned into a Macintosh computer, and densitometry was performed using the program NIH Image 1.5b2.

Thermal Melting Data Collection and Analysis. Hairpin or duplex samples were diluted to 2.0 × 10^{-6} M in either Pipes-00 or Pipes-10 at the indicated pH to a final volume of 1 mL. The samples were allowed to equilibrate to 15 °C for 0.5 h before melting. Thermal melting studies were performed in reduced-volume quartz Hellma 114B-QS self-masking cuvettes of 1 cm path length.

Data collection was performed using a Cary 3 UV–vis spectrophotometer. Absorbance data from the Cary 3 was collected on an IBM PS/2 Model 30 286 interfaced to the Cary 3 through a National Instruments IEEE-488 GPIB interface board and cable. The temperature was controlled and monitored by a Peltier temperature controller (Varian) from a starting temperature of 15 °C to a final temperature of 90 °C, at the rate of one 0.5 °C increment per minute. Absorbance readings were taken every 0.0333 s to produce an averaged value every 12 s for each cell. One averaged absorbance value was recorded every 0.5 °C increment and plotted as a function of temperature. In all cases, the reversibility of oligonucleotide melting was confirmed, and melting data were derived from 2–4 independent melting experiments.

The data were exported to a Macintosh IIci, where they were manipulated and visualized using the data analysis program KaleidaGraph (Synergy Software, Reading, PA). The melting transition temperature (T_m, °C) was determined as the inflection point of the absorbance versus temperature curve, corresponding to the rate of maximum absorbance change. If we assume a simple two-state model for melting, the first derivative of the melting curve is a Gaussian distribution with the maximum of the curve corresponding to the T_m. When the Gaussian distribution is perfectly symmetrical, the maximum also corresponds to the temperature at which 50% of the duplex hydrogen bonding is denatured.

For some oligonucleotide strands that have a high purine content, we observe a high-temperature melting transition due to single-stranded unstacking (Saenger, 1988), which interfered with accurate determination of the fraction of melted strand or duplex. Since the high-temperature transition was resolved from and independent of either a hairpin to strand transition or a duplex to strand transition, we employed a reintegration technique to separate transitions and to eliminate interference. A single Gaussian distribution was fit to the curve, omitting the high-temperature portion of the curve (>10 °C beyond T_m) that included the single-stranded stacking to unstacking transition. The calculated Gaussian distribution that corresponded to the melting transition was integrated numerically to yield a calculated absorbance curve for duplex to strand or hairpin to strand melting. The reintegrated absorbance curve was rescaled from 0 to 100 to represent the percentage of denaturation for each temperature point.

Kinetics Data Collection and Analysis. The instrumentation and data averaging used for the hairpin to duplex kinetics data collection are as described earlier for the thermal melting data collection. Hairpin oligonucleotides were diluted independently to 1.4×10^{-6} M in Pipes-00 or Pipes-10, adjusted to the indicated pH. For the pseudo-first-order experiments, one of the two samples was diluted to 7.0×10^{-6} M, which is 5 times the concentration of the other sample. Each 1 mL hairpin sample was placed in a separate chamber of a Hellma 238-QS quartz mixing cell and equilibrated to the appropriate temperature. After temperature equilibration, the cuvette was inverted to ensure complete mixing of the two samples. Mixing diluted the samples by another 2-fold as each 1 mL sample was diluted to a final volume of 2 mL. The final concentrations for standard and pseudo-first-order samples were 0.7×10^{-6} and 3.5×10^{-6} M, respectively. Absorbance data were collected as a function of time at a rate of one data point every 12 s. Kinetic curves from 2–4 experiments were analyzed as described below.

The data were exported to KaleidaGraph for manipulation and visualization. Rate constant determination was performed using a nonlinear least-squares analysis, an application of the Levenberg–Marquadt method (Press et al., 1992). The equation used in the curve-fitting routine (eq 1) is a modified form of a second-order equation (Jencks, 1975) that describes the rate of product formation from two equimolar components:

$$\mathrm{abs} = \mathrm{abs}_0 \frac{\epsilon_{\mathrm{duplex}}}{\epsilon_{\mathrm{AC}} + \epsilon_{\mathrm{GT}}} + \left(1 - \frac{\epsilon_{\mathrm{duplex}}}{\epsilon_{\mathrm{AC}} + \epsilon_{\mathrm{GT}}}\right)\left(\frac{\mathrm{abs}_0}{1 + [\mathrm{abs}_0/(\epsilon_{\mathrm{AC}} + \epsilon_{\mathrm{GT}})]kt}\right) \quad (1)$$

where abs is the absorbance, abs_0 is the measured absorbance at the initiation of the reaction, k is the rate constant, t is the time in minutes, and $\epsilon_{\mathrm{duplex}}$, ϵ_{AC}, and ϵ_{GT} are the ϵ_{260}'s for the duplex, the AC strand, and the GT strand, respectively. All parameters are fixed except the rate constant k. In some cases, we let $\epsilon_{\mathrm{duplex}}$ vary as well. In all cases, fitting $\epsilon_{\mathrm{duplex}}$ yielded a value similar to the input and had no effect on the fitted value for k. The correlation coefficient, R, and an unnormalized χ^2 were calculated by KaleidaGraph. A fixed standard deviation was derived from the instrument noise (±0.000 05 absorbance units) averaged over several experiments. χ^2 values were then divided by the number of data points and the standard deviation squared to yield normalized χ^2 values.

In order to determine the dependence of each hairpin on the rate of the hairpin to duplex transition, a modification of pseudo-first-order reactions was performed. Under conditions of excess reactant (a 10-fold excess of one component is standard for pseudo-first-order reactions), we observe a homoduplex side reaction. Consequently, the excess hairpin concentration was limited to 3.5×10^{-6} M, an excess of only 5-fold. As a 5-fold excess does not satisfy pseudo-first-order conditions, we utilized a modified form of a second-order equation that describes the rate of product formation from two components of unequal concentration (Jencks, 1975):

$$\mathrm{abs} = \mathrm{H1}_0(\epsilon_{\mathrm{P}} - \epsilon_{\mathrm{H2}}) + \mathrm{H2}_0\epsilon_{\mathrm{H2}} + \frac{\mathrm{H1}_0 - \mathrm{H2}_0}{1 - \mathrm{H2}_0 e^{-\mathrm{H1}_0 kt}/\mathrm{H1}_0 e^{-\mathrm{H2}_0 kt}}(\epsilon_{\mathrm{H1}} + \epsilon_{\mathrm{H2}} - \epsilon_{\mathrm{P}}) \quad (2)$$

where abs is the absorbance, $\mathrm{H1}_0$ and $\mathrm{H2}_0$ are the calculated initial concentrations of the hairpins, k is the rate constant, t is the time in minutes, and ϵ_{P}, ϵ_{H1}, and ϵ_{H2} are the ϵ_{260}'s for the duplex product and the hairpin reactants, respectively. Curve fitting was performed as described for eq 1.

A simple method for verifying the order of a reaction was devised by Wilkinson (1961). The reaction time divided by the fraction of duplex (t/f) is plotted as a function of time. Up to a duplex fraction of 0.4, the data fit to a straight line with a slope that is equal to the reaction order divided by 2. Beyond a duplex fraction of 0.6, the slope of any reaction approaches 1, which was used as a test to determine that the duplex fraction was calculated correctly. Using the t/f test, simulated first-order curves, second-order curves in which the reactants are of unequal concentrations (one reactant is in 5-fold excess), and second-order curves in which the reactants are of equal concentrations yield calculated theoretical orders of 1.1, 1.3, and 2.0, respectively. All measured curves were tested using the t/f test to verify the order, and we accepted only values that were within 10% of the predicted values. The results for second-order reactions were always 2.0. For the near pseudo-first-order conditions in which one of the hairpins is in 5-fold excess, we observed values of 1.3, which is almost identical to the predicted value. These results indicated that

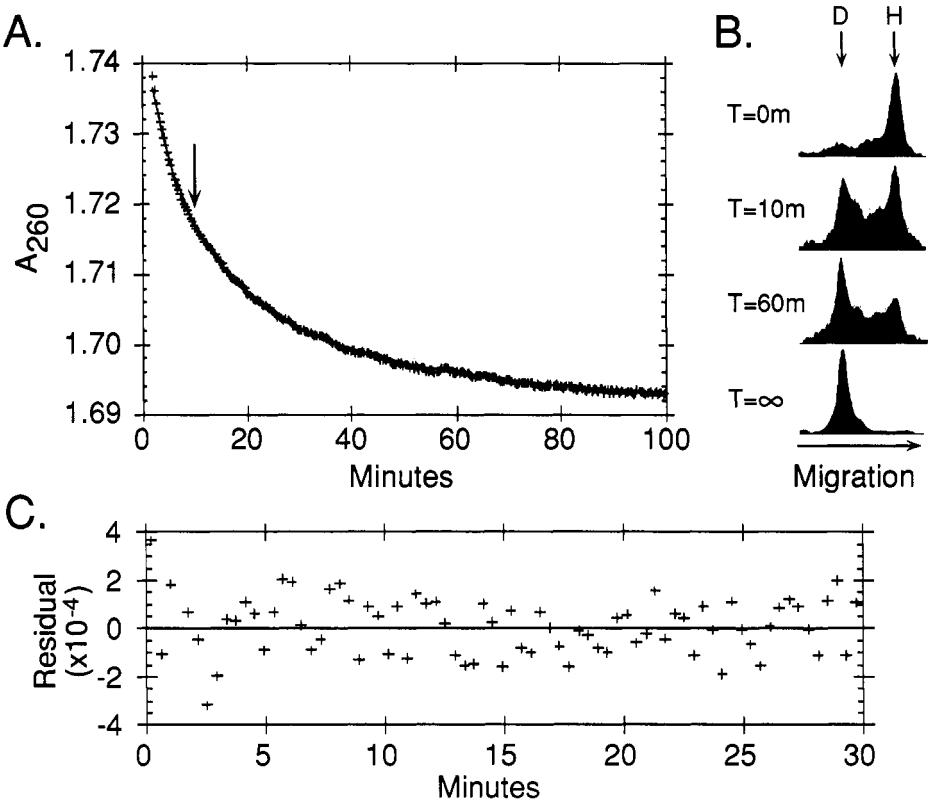

FIGURE 2: Time course of the hairpin to duplex transition. For both A and B, the starting concentration of each hairpin was 4×10^{-6} M (oligonucleotide) in 10 mM Pipes, 0.1 mM EDTA, and 80 mM NaCl at pH 7.0. The duplex is formed by mixing equal amounts of the AC and GT oligonucleotides at a fixed temperature (37 °C). (A) Formation of duplex measured by the decrease in the absorbance at 260 nm as a function of time (minutes). The arrow indicates the $t_{1/2}$ of the reaction, calculated from a second-order fit (—) to the data (+). (B) Densitometry trace of polyacrylamide gel electrophoresis results at various times during duplex formation. D indicates the duplex and H indicates the hairpin. Times are reported in minutes after AC and GT mixing. $T = \infty$ refers to a duplex 24 h after mixing. The arrow indicates the direction of electrophoretic migration. (C) Representative residual plot calculated from a second-order fit to the data (+). In this experiment, the starting concentration of each hairpin was 7×10^{-7} M in Pipes-10, and the reaction was carried out at 37 °C. The calculated rate constant for this reaction is reported in Table 1.

the 5-fold excess second order has an effective order between first and second order.

RESULTS

Duplex Formation from Equimolar Hairpin Mixing Is a Second-Order Process. Starting from a pure population of complementary hairpins (GT and AC), mixing results in an immediate decrease in absorbance that progresses over several hours. A representative plot of absorbance versus time at 37 °C in 10 mM Pipes, 0.1 mM EDTA, and 80 mM NaCl (pH 7.0) is shown in Figure 2A. We have recently reported that the structure of the GT hairpin contains a 3-member loop and a 10-bp stem (McMurray et al., 1994a; Spiro et al., 1993). The observed decrease in absorbance (hypochromicity) and its magnitude (~3%) are consistent with the small change that would occur as a result of stacking a 3-bp loop from each hairpin into a double-stranded duplex structure. The loop represents roughly 10% of the hairpin, and the hypochromicity value for a denatured strand to duplex transition is approximately 30% (Geiduschek, 1962).

To ensure that the absorbance decrease was due to duplex formation and to ensure the integrity of our starting material, we monitored the conformational state of the sample at several time points during the reaction using gel electrophoresis. Pure populations of the GT and AC hairpins were equilibrated and mixed at 37 °C for various times in 10 mM Pipes, 0.1 mM EDTA, and 80 mM NaCl (pH 7.0). The reactions were analyzed on 12% polyacrylamide gels, and the relative fraction of hairpin or duplex was measured by densitometry. Figure 2B shows the densitometry trace of individual lanes from the gel electrophoresis analysis of the hairpin sample before and at selected time points after mixing. We found that the relative fraction of hairpin and duplex corresponded well with the observed decrease in absorbance (Figure 2A). At the start of the reaction, all of the oligonucleotide is in the hairpin configuration. [Thermal melting data (see Figure 4) confirm that, at 37 °C, the individual oligonucleotides exist primarily as hairpins at pH 7.0.] At 10 min, we observed half of the total absorbance decrease, and the amounts of hairpin and duplex measured by densitometry are roughly equal. At 60 min, most of the hairpin has formed duplex, and after 24 h, essentially all of the oligonucleotide is in the duplex form.

To determine the rate of the reaction, the data points were fit to two models: a single first-order process that might indicate hairpin opening as the rate-limiting step, and a second-order model that might indicate nucleation as the rate-limiting step. In most cases, two parameters, rate constant and product extinction coefficient, were determined by the fit. Fitting only the rate constant (using a calculated value for the product extinction coefficient) had no significant effect on the value or quality (χ^2 or correlation coefficient) of the fitted rate constant. We were unable to obtain a good fit of the data to a single first-order process. However, as shown in Figure 2C, the data fit well to a second-order reaction in which each reactant is present at equal concentrations. Typical of second-order reactions (Figure 2A), the curve slowly approaches a final absorbance value, while residual plots (Figure 2C) and χ^2 values (Table 1) confirm the quality of the fit. The data

Table 1: Ionic Strength and pH Dependence of the Hairpin to Duplex Transition at 37 °C[a]

[Na+]	pH	k (M^{-1} s^{-1})	χ^2	R[d]	%H[e]
Pipes-00 (0.015 M)[b]	6.0	140	1.8	0.9938	2.9
	7.0	350	1.5	0.9927	2.1
	8.0	1200	1.3	0.9993	5.8[f]
Pipes-10 (0.1 M)[c]	6.0	4000	1.6	0.9920	2.1
	7.0	7300	1.1	0.9978	3.1
	8.0	9800	2.9	0.9957	4.5

[a] Summary of the rate constants of the hairpin to duplex transition. For each reaction, 0.7 μM AC and GT oligonucleotides in 1 mL each are mixed to form a double-stranded heteroduplex. [b] Na^+ concentration is calculated by the amount of NaOH used to titrate Pipes-00 (10 mM Pipes, 0.1 mM EDTA) to the proper pH. [c] Pipes-10 (10 mM Pipes, 0.1 mM EDTA, and 100 mM NaCl). [d] The correlation coefficient R. [e] Hypochromicity change (absorbance decrease) from reaction initiation to the calculated reaction completion. [f] Larger hypochromicity change due to a high amount of single-stranded AC oligonucleotide at pH 8.0.

deviate from the calculated curve fit only in a random fashion, and the fit has a χ^2 of 1.1 and a correlation coefficient of 0.9978. We found that the hairpin to duplex transition of the proenkephalin enhancer occurs slowly. At micromolar concentrations, the half-life of the reaction at 37 °C in Pipes-10 at pH 7.0 is about 4 min, and the best fit value for the rate constant of the hairpin to duplex reaction was 7300 M^{-1} s^{-1} (see Table 1).

Duplex Formation Is Highly Dependent on pH and Ionic Strength. We have previously reported that the duplex to hairpin transition is pH dependent. In the range 6.0–8.0, decreasing the pH increases the stability of the AC hairpin and shifts the hairpin/duplex enhancer equilibrium toward the hairpin form (McMurray et al., 1991). To determine whether alteration of the pH also affects the kinetics of this process, we measured the rate of duplex formation that occurs upon mixing hairpins under different pH conditions. The pH dependence of duplex formation was measured by the absorbance change under both low (Pipes-00) and high ionic strength (Pipes-10) at 37 °C. The values of the rate constants for the best second-order fit to the data are reported in Table 1. We found that the rate of formation of the enhancer duplex was directly proportional to both the pH and the ionic strength. In Pipes-00, lowering the pH from 8.0 to 6.0 decreased the half-life of duplex formation from 190 to 30 min. Thus, the effect of pH on the rate of duplex formation is large if the enhancer is in a low ionic strength environment. At high ionic strength, the rate of duplex formation is still dependent on pH, but the effect is smaller. In Pipes-10, lowering the pH decreases the half-life of duplex formation from 10 to 3 min. At all pH conditions in Pipes-10, reactions proceed at a rate roughly an order of magnitude faster than reactions in Pipes-00.

The AC Hairpin Is the Rate-Limiting Reactant at Low pH. Since the pH has a large effect on the relative stabilities of the hairpins, we determined whether, under different pH conditions, a particular hairpin was governing the rate of duplex formation. The dependence of the rate of duplex formation on each individual hairpin can be determined by using pseudo-first-order conditions; one hairpin is in large excess compared to the other (Jencks, 1975). However, we observed that if either oligonucleotide was present in large excess, some homoduplex formation occurred. (Thus, it was not possible to achieve truly pseudo-first-order conditions without interference from the second transition.) For these experiments, the concentration of the excess hairpin was present in 5-fold excess, so that its concentration changes by less than 20% over the course of a reaction. To analyze these curves, we fit the second-order equation that describes the rate of duplex formation when the reactants are of unequal concentrations (Experimental Procedures). In these experiments, the concentration of the limiting hairpin is identical to the concentration of hairpin used to generate the curves analyzed in Table 1.

Table 2: Effect of Each Hairpin on the Hairpin to Duplex Transition in Pipes-00 at 37 °C[a]

pH		k (M^{-1} s^{-1})	χ^2	R[c]
6.0	AC > GT[b]	220	2.5	0.9954
	AC = GT	140	1.8	0.9938
	GT > AC	140	2.1	0.9782
7.0	AC > GT	540	1.8	0.9978
	AC = GT	350	1.5	0.9927
	GT > AC	400	3.9	0.9938

[a] Summary of the rate constants of the hairpin to duplex transition, fit to data shown in Figure 3. [b] AC > GT indicates that the AC hairpin is in 5-fold excess. AC = GT indicates that the hairpins are of equal concentrations. GT > AC indicates that the AC hairpin is in 5-fold excess. [c] The calculated correlation coefficient.

The effect of altering individual hairpin concentrations on duplex formation at 37 °C in Pipes-00 is shown in Figure 3. The excess hairpin reactions have two features that distinguish them from the equal concentration reactions and suggest that when one hairpin is in 5-fold excess the conditions are close to pseudo-first order. First, the velocity of the reaction when one hairpin is in 5-fold excess is much higher than the velocity of the reaction when both hairpins are at equal concentrations. This is expected since a second-order velocity is dependent on the concentrations of both reactants. Second, the excess hairpin curves have a much flatter plateau after the half-life, indicating the first-order character of the reactions. The order of the reactions was verified using a simple t/f test (Wilkinson, 1961; see Experimental Procedures). We found that the t/f test results for the order of the excess hairpin curves were about 1.2–1.3, which is close to the predicted value for a pseudo-first-order reaction. As expected, the t/f test yielded a value of 2 for reaction order for mixing the hairpins at equal concentrations. Thus, a reaction with only a 5-fold excess of one reactant reasonably approximates pseudo-first-order conditions, and the dependence of the reaction on individual hairpins can be determined under these conditions.

Table 2 compares the calculated rate constants for the experiments shown in Figure 3. At both pH 6.0 and 7.0, the reaction in which the GT hairpin is limiting proceeds at a faster rate (about 1.5 times) than the equal concentration reaction, indicating that the reaction is more dependent on the AC hairpin. When the AC hairpin is limiting, the fitted rate constant for the hairpin to duplex reaction is virtually indistinguishable from the rate constant when reactants are at equal concentrations. Thus, the hairpin to duplex reaction depends on the AC hairpin at pH values between 6.0 and 7.0. The data indicate that the dominance of the AC hairpin increases as the pH decreases.

Duplex Formation Is a Two-State Process over a Limited Temperature Range. As expected, enhancer duplex formation in Pipes-10 at pH 7.0 is temperature dependent. Increasing the temperature from 25 to 40 °C results in an 18-fold decrease in the half-life of the reaction (not shown). At 25 °C, the half-life is 60 min and the rate constant is 405 M^{-1} s^{-1}, while at 40 °C, the half-life is approximately 3 min with a rate constant of 7300 M^{-1} s^{-1}]. Second-order rate constants determined from equal concentration reactions at various temperatures were used to determine the activation energy of the hairpin to duplex reaction under the different pH and ionic strength conditions.

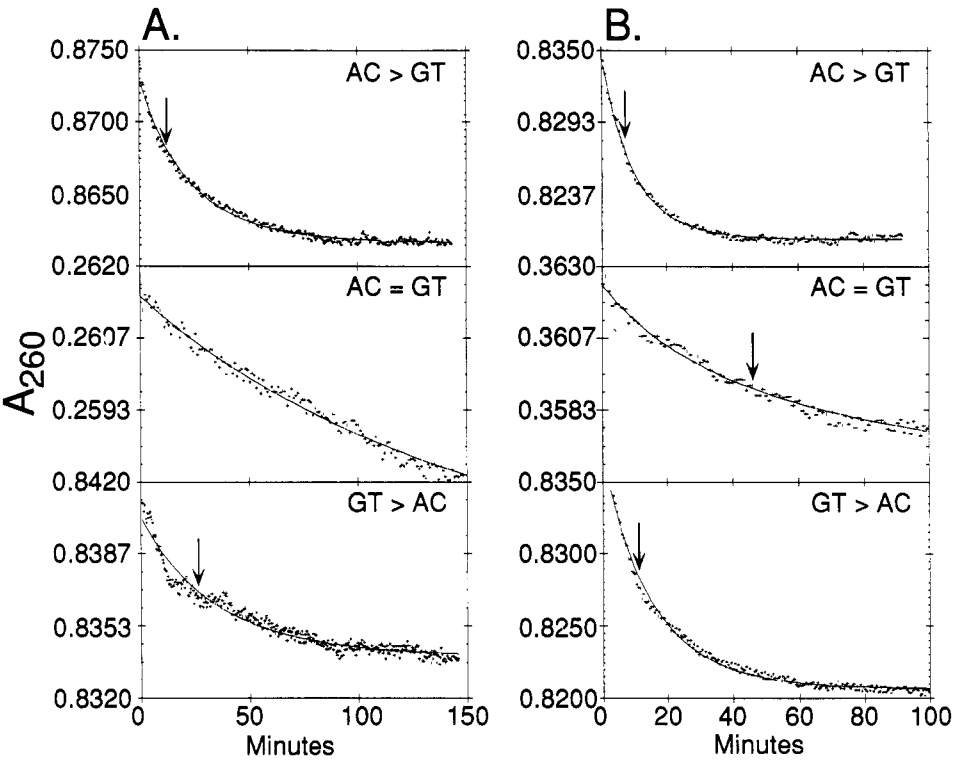

FIGURE 3: Effect of individual hairpins on the rate of the hairpin to duplex reaction in Pipes-00 at (A) pH 6.0 and (B) pH 7.0, measured by the change in absorbance at 260 nm as a function of time in minutes. In the top curve of each column (AC > GT), the concentration of the AC hairpin is 3.5×10^{-6}M and the concentration of the GT hairpin is 7×10^{-7}M. In the middle curves (AC = GT), the concentration of each hairpin is 7×10^{-7}M. In the bottom curves (GT > AC), the concentration of the GT hairpin is 3.5×10^{-6}M and the concentration of the AC hairpin is 7×10^{-7}M. The arrows indicate the $t_{1/2}$ of the reaction, calculated from a second-order fit (—) to the data (+). At pH 6.0, AC = GT, the $t_{1/2}$ is past the display range. Rate constants are reported in Table 2.

The activation energy is determined from the slope of the rate constants plotted against the reciprocal temperature using the Arrhenius relationship (eq 3). However, physical meaning for the Arrhenius relationship depends on the maintenance of a two-state process over the entire temperature range of the measurements. Since we had previously shown that the stability of each hairpin is highly pH dependent (McMurray et al., 1991), it was necessary to define conditions for which the oligonucleotides remained primarily in the hairpin conformation.

The percentage of hairpin for both the GT and AC oligonucleotides under different pH and ionic strength conditions was determined by thermal melting analysis. We found that the fraction of hairpin could not be accurately determined from the T_m curves directly, due to a high-temperature unstacking transition that occurs in purine-rich strands (Saenger, 1988). To accurately determine the percent of hairpin, the T_m's of each oligonucleotide were calculated from the first derivative of the data, fit to a Gaussian distribution using data points up to but not including the high-temperature unstacking transition. An example of the fit for the AC oligonucleotide in Pipes-10 (pH 7.0) is shown in the inset of Figure 4. The T_m (arrow A) is the peak of the Gaussian distribution, and the last data point used to calculate the Gaussian distribution is arrow B. The Gaussian distribution is extrapolated to zero on both sides, integrated numerically, and normalized to a range of 0–100, indicating the percentage of melted strand. The percentage of hairpin is the calculated percentage of melted strand subtracted from 100%.

The percentages of hairpin determined from thermal melting analysis for the AC and GT oligonucleotides in Pipes-10 at pH 6.0, 7.0, and 8.0 are shown in Figure 4. The T_m and broadness of the GT hairpin transition are insensitive to

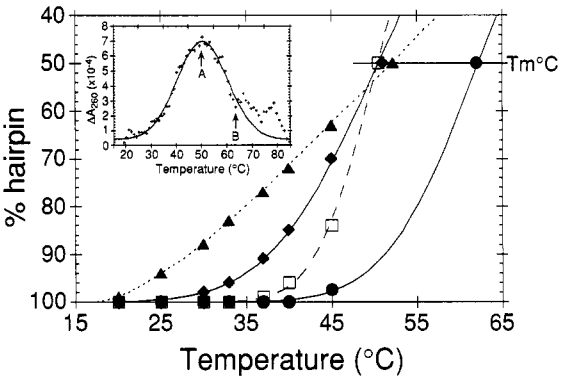

FIGURE 4: pH dependence of thermal melting for the GT hairpin and AC hairpin in Pipes-10. The inset is a sample curve demonstrating the method of curve calculation shown in the main figure, the first derivative of the AC melting curve at pH 7.0 (+) with the calculated Gaussian distribution (—). The starting concentration of the AC hairpin was 7×10^{-7} M. Arrow A is the calculated T_m of 50.1 °C. Arrow B indicates the upper limit of the data (63.5 °C) used to determine the Gaussian distribution (see Experimental Procedures). In the main figure, the calculated curves are shown for the AC hairpin at pH 6.0 (●) and 7.0 (◆) and for the GT hairpin at pH 6.0, 7.0, and 8.0 (□, – –), measured by the percent of free strand as a function of temperature. The AC curve at pH 8.0 (▲, - - -) is a percentage normalization of the raw absorbance data. The symbol at 50% strand indicates the T_m for each hairpin, and the other symbols indicate temperatures at which duplex formation experiments were performed.

changes in pH, so the percentages of hairpin at pH 6.0, 7.0, and 8.0 are identical. In the temperature range from 20 to 45 °C, the percentage of GT hairpin was relatively unchanged, ranging from 100% to 85%. As previously reported (McMurray et al., 1991), the T_m of the AC oligonucleotide is highly sensitive to pH changes, so that significant fluctuations in the amount of free strand can occur with small changes in

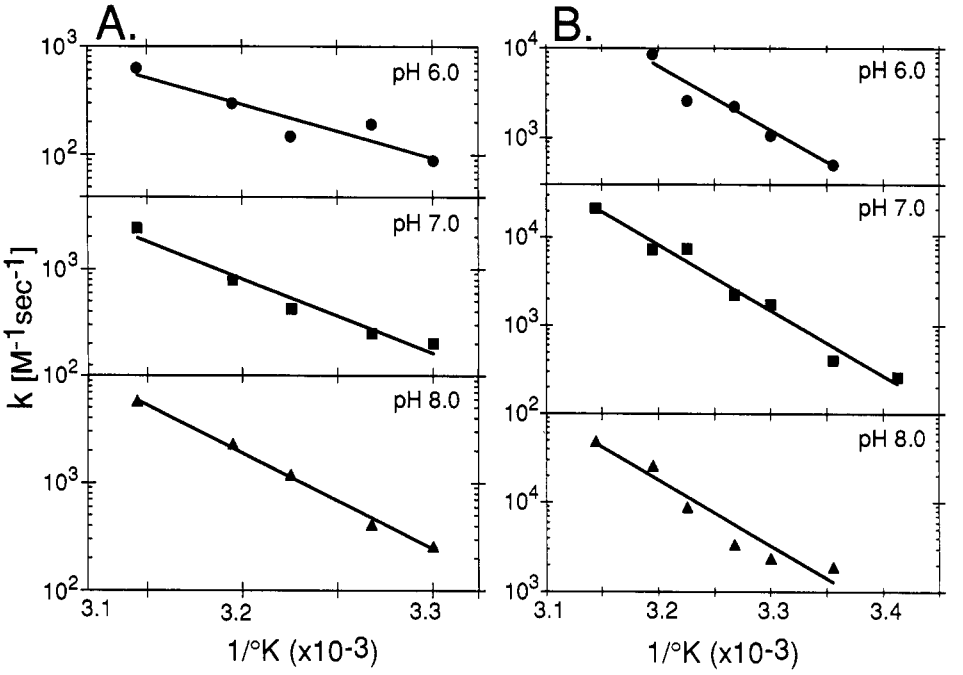

FIGURE 5: Arrhenius plots of the hairpin to duplex transition as a function of pH and ionic strength. The activation energy is determined by the slope of the rate constant (M^{-1} sec^{-1}) as a function of reciprocal absolute temperature (1/K) (eq 3). For all points, the starting concentration of the hairpins was 7×10^{-7} M at pH 6.0 (●), 7.0 (◆), and 8.0 (▲) in Pipes-00 (A) and Pipes-10 (B). The activation energies calculated from the slopes are reported in Table 3.

pH. At pH 6.0, the AC hairpin is very stable, with a T_m of 62 °C. As a result, the AC oligonucleotide is almost 100% hairpin (free strand is <2%) in the 20–45 °C range. At pH 7.0, approximately 86% of the AC oligonucleotide remains in the hairpin form at 40 °C, but at 45 °C the percentage of hairpin decreases to 70%. At pH 8.0, the curve for the AC hairpin was normalized from the raw absorbance data, as a Gaussian distribution did not fit well to the data. At all temperature points, the amount of strand at pH 8.0 for the AC oligonucleotide is much higher than those found for the GT oligonucleotide and the AC oligonucleotide at other pH values. At pH 8.0, only 76% of the AC oligonucleotide is in the hairpin form at 37 °C.

The data indicate that 40–45 °C is the upper limit for observing the rate of the hairpin to duplex reaction. Above this temperature, the significant fraction of denatured strand had large effects on the calculated rate constant and the linearity of the Arrhenius plot (data not shown). While the high-temperature experiments are limited by the increasing amount of free strand, temperature experiments below 20 °C were limited by a tendency of the GT oligonucleotide to form a homoduplex structure. At low temperatures (below 15 °C), the hairpin to duplex reactions did not reach completion after several hours, during which time the GT homoduplex became more prominent (data not shown). These results were used to define a temperature range valid for studying the hairpin to duplex reaction rates. On the basis of the thermal melting data, we limited our Arrhenius plot to rate constants measured between 20 °C and 45 °C.

The Activation Energy of Duplex Formation Is Dependent on pH and Ionic Strength. The activation energy is determined from the Arrhenius equation:

$$k = Ae^{-E_a/RT} \quad (3)$$

where k is the hairpin to duplex rate constant determined for a reaction at T, the absolute temperature. E_a is the activation energy, R is the gas constant, and A is a "collision factor"

Table 3: Effect of Ionic Strength and pH on the Activation Energy of the Hairpin to Duplex Transition[a]

[Na^+]	pH	E_a (kcal/mol)	R^b
Pipes-00 (0.015 M)	6.0	22.4	0.968
	7.0	31.8	0.989
	8.0	40.8	0.998
Pipes-10 (0.1 M)	6.0	32.5	0.946
	7.0	33.9	0.989
	8.0	33.8	0.987

[a] The activation energy determined from the Arrhenius equation (eq 3) fit to the data in Figure 5. [b] The calculated correlation coefficient.

(Jencks, 1975). To determine the activation energy, we plotted the rate constants as a function of temperature at temperature intervals of roughly 5 °C between 20 and 45 °C (including 37 °C). The fraction of hairpin at every temperature point utilized for the activation energy plot is indicated with symbols in the thermal melting profiles in Figure 4. The natural logarithms of the measured rate constants were plotted versus reciprocal temperature (1/K) for reactions in Pipes-00 (Figure 5A) and Pipes-10 (Figure 5B) at pH 6.0, 7.0, and 8.0.

The activation energy for a given pH and ionic strength can be calculated from the slope of the appropriate Arrhenius plot in Figure 5. The calculated activation energies are reported in Table 3. Under low ionic strength conditions (Pipes-00), the activation energy of the hairpin to duplex reaction is affected by pH (Table 3), increasing by roughly a factor of 2, from 22.4 to 40.8 kcal/mol between pH 6.0 and 8.0. Under high ionic strength conditions (Pipes-10), pH has little effect on the rate of the hairpin to duplex transition. The slopes of the lines determined by the Arrhenius equation (eq 3) are almost completely parallel, indicating that the activation energy is insensitive to changes in pH under physiological ionic strength conditions. The activation energies in Pipes-10 are virtually identical at pH 7.0 and 8.0 and less than 5% smaller at pH 6.0.

DISCUSSION

The change in the secondary structure of the human enkephalin enhancer from a linear duplex to a cruciform of two hairpins has been implicated in the transcriptional control of the enkephalin gene. For the enhancer cruciform to be a regulatory switch, it must satisfy at least two criteria. First, the transition must be reversible, and second, both the duplex and the hairpin states must have reasonable lifetimes in solution. Our measurements indicate that the hairpin to duplex transition of the proenkephalin enhancer satisfies both of these criteria. We have previously shown that the hairpin to duplex transition of the proenkephalin enhancer is reversible and dependent on pH (McMurray et al., 1991). Under low oligomer concentrations, the hairpin state is favored at pH 6.0 and the duplex state is favored at pH 8.0. Under physiological ionic strength conditions, small decreases in the pH between 8.0 and 6.0 result in large changes in the rate of duplex formation at 37 °C, from $k = 4000$ to 10 000 M^{-1} s^{-1}. Under low ionic strength conditions, the rate of duplex formation is roughly 10–20 times slower, from $k = 140$ to 1200 M^{-1} s^{-1}. At pH 6.0 and low ionic strength, the hairpin to duplex transition is not complete even after 2 h. Therefore, conditions that alter the environment of the enhancer can have a dramatic influence on the lifetime of the hairpin state.

A factor that may alter both the local pH and the ionic strength environment of the enhancer is the binding of a charged protein. CREB, an important transcriptional regulator, binds to the hairpin form of the enhancer (Spiro et al., 1993). The N-terminus of CREB contains many acidic residues, a common motif of many transcriptional regulatory proteins. The frequent occurrence of acidic portions has indicated that these regions must have important functions (Mitchell & Tjian, 1989). Additionally, CREB's ability to regulate transcription is phosphorylation dependent (Brindle & Montminy, 1992). Although the spatial localization (with respect to DNA) of neither the phosphorylation site nor acidic residues is known, it is possible that one function of the acidic residues may be to locally lower the pH environment of the proenkephalin enhancer, slowing down the rate of return to the duplex state. Even in the absence of a stabilizing protein, the activation energy for the return to a duplex state is high (~32 kcal/mol). Thus, once the hairpin state forms, the hairpin state has a long lifetime even under conditions where the free energy difference between cruciform and duplex states favors the duplex. Under low ionic strength conditions (Pipes-00), a possible environment during protein association, the activation energy for return to the duplex state is high (22.4–40 kcal/mol) and is more sensitive to small changes in pH.

The activation energy for the forward reaction, formation of the hairpins from a stable duplex, will be higher than that for the reverse reaction at neutral pH. Thus, the probability of hairpin formation is small. However, at least two factors may lower the activation energy of the forward reaction. First, proteins may stabilize the hairpin state and facilitate the rate of hairpin formation. We know that CREB not only binds the GT hairpin it also stabilizes secondary structure in the proenkephalin enhancer (McMurray et al., 1994a). Direct imaging of a CREB/enkephalin gene complex demonstrates that CREB binding to a 1300-bp duplex containing a centrally located enkephalin enhancer induces an open state in the DNA at the enhancer region that becomes nuclease sensitive (McMurray et al., 1994b). Additionally, HMG1, and perhaps other conserved cellular proteins, specifically binds to cruciforms in a sequence-independent manner (Bianchi et al., 1989). Finally, negative supercoiling has been shown to facilitate the formation of cruciforms (Dayn et al., 1992; Mizuuchi et al., 1982).

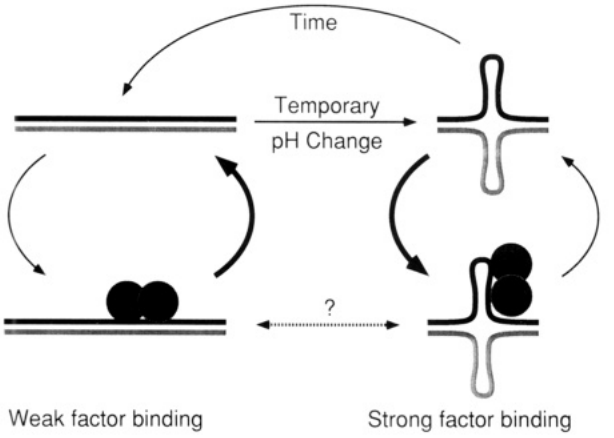

FIGURE 6: Model for the role of the hairpin to duplex DNA structural change in the control of transcriptional regulation.

We note that the measured activation energies for return to the duplex state from two stable hairpins, under any solution condition that we utilized, are large. The activation energy barrier under physiological conditions is equivalent to the energy released by the binding of a protein with an association constant of 1.4×10^{14} M^{-1}. However, we presume that this calculated activation energy is an overestimate of the actual value since we have not accounted for, in this initial study, either the cost of junction formation or the contribution of DNA length and flanking sequence (Sullivan & Lilley, 1986) to the rate of duplex formation. It is also important to note that our present *in vitro* studies deviate from the *in vivo* situation with respect to concentration dependence. Thus, we are currently extending kinetic studies utilizing longer, linked oligonucleotide templates that should more closely approximate *in vivo* reaction rates and energy costs.

Finally, we propose a model that describes how DNA hairpins with the properties of the proenkephalin enhancer might act as a switch for transcriptional regulation (Figure 6). CREB, a constitutive factor in the brain and many other cell types, preferentially binds and stabilizes the hairpin form of the enhancer. The linear duplex is inherently a poor binding site for CREB, but the low affinity of CREB for the duplex form may serve a function in targeting CREB to the enhancer. CREB facilitates enhancer opening and hairpin formation. This function may be aided by the acidic portions of the CREB protein and/or by phosphorylation that locally increases the net negative charge environment of the enhancer. We have shown that small decreases in pH can induce protonation of the AC hairpin and increase its stability (McMurray et al., 1991). Additionally, pseudo-first-order conditions indicate that the AC hairpin is the rate-limiting reactant in duplex formation. Thus, CREB binding and the acidic environment of the CREB/enhancer complex may play a role in stabilizing both the GT and AC hairpins. In this model, the GT hairpin acts as the substrate for CREB binding, while the AC hairpin might regulate the existence of the CREB binding site in the GT hairpin and the overall stability of the cruciform state.

The CREB/hairpin complex may serve to increase or decrease the rate of transcription. Hairpin formation could provide a favorable conformation for CREB to interact with the polymerase complex (Hai et al., 1988; Horikoshi et al., 1988). Alternatively, CREB may aid in transcriptional initiation, but inhibit elongation as long as the hairpin is present. Proenkephalin mRNA levels in the hippocampus upon kainate treatment only reach a maximum 12–24 h after

stimulation (Douglass et al., 1991). Hairpin formation can take up energy needed for a closed to open promoter complex transition (von Hippel et al., 1984). The high activation energy indicates that two stable hairpins are resistant to relaxing back to the linear duplex form. Thus, whatever the effect, the slow rate of relaxation and a high activation energy for duplex formation indicate that the enhancer can exert its effect (positive or negative) for a finite time after termination of the hairpin-stabilizing event. The magnitude of the activation energy may suggest that, once the hairpin forms, return to the duplex state requires additional energy, perhaps provided by a protein binding event.

We conclude that DNA hairpin formation can be a mechanism for an additional level of transcriptional control since the existence of the hairpin partially decouples the probability and the rate of transcription from the presence or absence of transcriptional proteins. The lifetime of the hairpin may control the timing of transcription by governing the existence of DNA conformations or protein binding sites required for successful initiation and/or elongation.

ACKNOWLEDGMENT

We thank Craig Spiro, Jane Collins-Hicok, David Wilson, and Fariel Tanious for discussion and helpful suggestions.

REFERENCES

Bazett-Jones, D. P., & Brown, M. L. (1989) *Mol. Cell. Biol. 9*, 336–41.

Bianchi, M. E., Beltrame, M., & Paonessa, G. (1989) *Science 243*, 1056–1059.

Brennan, R. G., Roderick, S. L., Takeda, Y., & Matthews, B. W. (1990) *Proc. Natl. Acad. Sci. U.S.A. 87*, 8165–8169.

Brindle, P. K., & Montminy, M. R. (1992) *Curr. Opin. Genet. Dev. 2*, 199–204.

Cantor, C. R., & Tinoco, I., Jr. (1965) *J. Mol. Biol. 13*, 65–77.

Cantor, C. R., Warshaw, M. M., & Shapiro, H. (1970) *Biopolymers 9*, 1059–1077.

Chory, J. (1993) in *Current Protocols in Molecular Biology* (Ausubel, F. M., Brent, R., Kingston, R. E., Moore, D. D., Seidman, J. G., Smith, J. A., & Struhl, K., Eds.) pp 2.7.1–2.7.5, Greene/Wiley Interscience, New York.

Comb, M., Birnberg, N. C., Seasholtz, A., Herbert, E., & Goodman, H. M. (1986) *Nature (London) 323*, 353–356.

Comb, M., Mermod, N., Hyman, S. E., Pearlberg, J., Ross, M. E., & Goodman, H. M. (1988) *EMBO J. 7*, 3793–3805.

Dayn, A., Malkhosyan, S., & Mirkin, S. (1992) *Nucleic Acids Res. 20*, 5991–5997.

Douglass, J. O., Iadarola, M. J., Hong, J. S., Garrett, J. E., & McMurray, C. T. (1991) *NIDA Res. Monogr.* 133–148.

Geiduschek, E. P. (1962) *J. Mol. Biol. 4*, 467–487.

Giraud, P., Kowalski, C., Barthel, F., Becquet, D., Renard, M., Grino, M., Boudouresque, F., & Loeffler, J. P. (1991) *Neuroscience 43*, 67–79.

Glucksmann, M. A., Markiewicz, P., Malone, C., & Rothman-Denes, L. B. (1992) *Cell 70*, 491–500.

Goodman, R. H. (1990) *Annu. Rev. Neurosci. 13*, 111–127.

Hai, T., Horikoshi, M., Roeder, R. G., & Green, M. R. (1988) *Cell 54*, 1043–1051.

Horikoshi, M., Hai, T., Lin, Y. S., Green, M. R., & Roeder, R. G. (1988) *Cell 54*, 1033–1042.

Horwitz, M. S. Z., & Loeb, L. A. (1988) *Science 241*, 703–705.

Huggenvik, J. I., Collard, M. W., Stofko, R. E., Seasholtz, A. F., & Uhler, M. D. (1991) *Mol. Endocrinol. 5*, 921–930.

Jencks, W. P. (1975) in *Catalysis in Chemistry and Enzymology* pp 605–612, Dover, New York.

Kerppola, T. K., & Curran, T. (1991) *Science 254*, 1210–1214.

Kobierski, L. A., Chu, H. M., Tan, Y., & Comb, M. J. (1991) *Proc. Natl. Acad. Sci. U.S.A. 88*, 10222–10226.

Konradi, C., Kobierski, L. A., Nguyen, T. V., Heckers, S., & Hyman, S. (1993) *Proc. Natl. Acad. Sci. U.S.A. 90*, 7005–7009.

Lyubchenko, Y., Shlyakhtenko, L., Chernov, B., & Harrington, R. E. (1991) *Proc. Natl. Acad. Sci. U.S.A. 88*, 5331–5334.

MacArthur, L., Koller, K. J., & Eiden, L. E. (1993) *Mol. Pharmacol. 44*, 545–551.

McMurray, C. T., Wilson, W. D., & Douglass, J. O. (1991) *Proc. Natl. Acad. Sci. U.S.A. 88*, 666–670.

McMurray, C. T., Juranic, N., Chandrasekaran, S., Macura, S., Li, Y., Jones, R. L., & Wilson, W. D. (1994a) *Biochemistry* (following article in this issue).

McMurray, C. T., Spiro C, Lin L., & Bazett-Jones, D. P. (1994b) *Proc. Natl. Acad. Sci. U.S.A.* (submitted).

Mitchell, P. J., & Tjian, R. (1989) *Science 245*, 371–378.

Mizuuchi, K., Mizuuchi, M., & Gellert, M. (1982) *J. Mol. Biol. 156*, 229–243.

Nickol, J., & Rau, D. C. (1992) *J. Mol. Biol. 228*, 1115–1123.

Pérez-Martín, J., & Espinosa, M. (1993) *Science 260*, 805–807.

Press, W. H., Teukolsky, S. A., Vetterling, W. T., & Flannery, B. P. (1992) in *Numerical Recipes in C*, pp 656–706, Cambridge University Press, New York.

Saenger, W. (1988) in *Principles of Nucleic Acid Structure* pp 194–215, Springer-Verlag, New York.

Sonnenberg, J. L., Rauscher, F. J., Morgan, J. I., & Curran, T. (1989) *Science 246*, 1622–1625.

Spiro, C., Richards, J. P., Chandrasekaran, S., Brennan, R. G., & McMurray, C. T. (1993) *Proc. Natl. Acad. Sci. U.S.A. 90*, 4606–4610.

Sullivan, K. M., & Lilley, D. M. J. (1986) *Cell 47*, 817–827.

von Hippel, P. H., Bear, D. G., Morgan, W. D., & McSwiggen, J. A. (1984) *Annu. Rev. Biochem. 53*, 389–446.

Wilkinson, R. W. (1961) *Chem. Ind. (London)*, 1395–1397.